Dynamic simulator for capillary electrophoresis with in situ calculation of electroosmosis

Richard A. Mosher[a], Chao-Xuan Zhang[b], Jitka Caslavska[b], Wolfgang Thormann[b],*

[a]Center for Separation Science, University of Arizona, Tucson, AZ 85721, USA
[b]Department of Clinical Pharmacology, University of Berne, Murtenstrasse 35, CH-3010 Berne, Switzerland

Abstract

A dynamic computer model for the simulation of open-tubular capillary electrophoresis which includes in situ calculation of electroosmosis along the capillary column is described. For each column segment, electroosmosis is calculated with the use of a wall mobility, the voltage gradient and the dissociation of the wall represented by the dissociation of a weak monovalent acid. Then, the bulk capillary flow is taken to be the average of all of the segment flows and considered to represent a plug flow. This simple approach permits the combined simulation of the temporal behavior of electroosmosis and electrophoresis. Comparison of simulation data obtained with a wall pK of about 6 and a mobility between $5 \cdot 10^{-8}$ and $7 \cdot 10^{-8}$ m^2/V·s with data produced in untreated fused-silica capillaries shows that the model provides a good estimate of the magnitude and distribution of electroosmosis when having buffers of pH > 5.5. For lower pH, a pK lower than 6 has to be used, this representing a rough approximation only. The model also provides the whole dynamics of all components, the electrical column properties, and emulated detector responses for direct and indirect optical, conductivity, pH and electrochemical detection at specified capillary locations.

1. Introduction

Computer simulation of electrophoresis has demonstrated considerable value as a research tool. Many examples of qualitative and even quantitative agreement between predictions and experimental results have confirmed the utility of simulations for the prediction of separability, separation dynamics, zone characteristics and boundary structure, and also for the reproduction and explanation of some experimentally observed phenomena. Although most of the simulation work performed so far was limited to quiescent solution [1–4], models which include

---

* Corresponding author.

imposed plug flow have been created, particularly to simulate the buffer and sample dynamics in open-tubular capillary electrophoresis [5–7] and in isotachophoresis with a counterflow [8].

In capillary electrophoresis, electrokinetic separations are carried out in capillaries or narrow-bore tubes having radii <0.5 mm. Instrumentation with open-tubular, fused-silica capillaries of very small I.D. (25–75 μm) is now available, in which electroosmotic and electrophoretic mass transport occur concomitantly. Electroosmosis thus plays a pivotal role in this process. It is dependent on surface charge (pH), the electric field determined by current density and conductivity (composition of the solutions present in the capillary) and viscosity. These

three parameters are typically constant in capillary zone electrophoresis in which the sample is the only discontinuous element present, but may vary in configurations consisting of discontinuous buffer systems, such as capillary isotachophoresis and capillary isoelectric focusing.

The dynamic computer model developed at the University of Arizona [1–3] was adapted for use on a PC [4] and has also been modified to allow more specific treatments of capillary electrophoresis, including the addition of imposed plug flow along the separation axis and emulation of solute monitoring along specified locations along the capillary [7]. With this approach, the temporal behavior of electroosmosis cannot be predicted based on the calculated dynamics of the column properties, and thus simulated sample and buffer dynamics are dependent on the flow parameters initially imposed. These shortcomings prompted an extension of the model to include in situ calculation of electroosmosis. In this paper, a simple model for computer simulation of electroosmosis in capillary electrophoresis which is based on the dissociation of the silanol surface groups of the capillary wall is described. It predicts (i) the temporal behavior of electroosmosis and (ii) the electroosmotic pumping activity of each fluid element (segment) along the capillary column at specified time points after power application and provides the whole dynamics of all components, pH, conductivity, voltage gradient, current density and column resistance.

2. Theoretical

The dynamic computer model has been described in detail previously [1–4,7]. In the interest of clarity, the major points are outlined here. The model is one dimensional and based on the principles of electroneutrality and conservation of mass and charge. Isothermal conditions are assumed and relationships between the concentrations of the various species of a component are described by equilibrium constants. The model is capable of treating biprotic ampholytes, weak and strong monovalent acids and bases and

proteins. Component fluxes are computed on the basis of electromigration and diffusion in quiescent solution [1–4] or in presence of an imposed constant or time-dependent plug flow along the separation axis [7]. Initial conditions which must be specified for a simulation include the distribution of all components, the diffusion coefficient and net charge–pH relationships of the proteins, the pK and mobility values of the buffer constituents, the current density or applied constant voltage, the flow constants, the duration of the current flow, the column length and its segmentation and the permeabilities of the ends of the separation space. The program outputs concentration, pH and conductivity profiles as functions of time and allows the presentation of these data either as profiles along the column at specified time intervals or as data which would be produced by a detector at a specified column location, i.e., segment number.

The model for capillary electrophoresis with superimposed plug flow [7] has now been extended with the option of the in situ calculation of electroosmosis along the capillary column. For each column segment i, electroosmosis is calculated with the use of a wall or absolute electroosmotic mobility, μ_0, the voltage gradient, E_i, and the degree of ionization of the wall, α_i:

$$v_{EO_i} = \mu_0 E_i \alpha_i \tag{1}$$

In the present approach, the dissociation of the silanol groups of the capillary surface was assumed to be the only contribution to surface charge. The wall dissociation is therefore that of a weak monovalent acid for which the degree of ionization is given by

$$\alpha_i = 10^{(pH_i - pK)} / [1 + 10^{(pH_i - pK)}] \tag{2}$$

where pK is the pK_a value of silanol (pK of the wall) and pH_i is the pH of the solution in the capillary segment. The degree of ionization varies from 0 to 1.

In analogy with Darcy's equation, which is valid for pressure-driven flow, the bulk capillary flow is taken to be the average of all of the segment flows, i.e. the electroosmotic velocity in

open tubular fused-silica capillaries is computed by

$$v_{EO} = \frac{1}{n} \sum_{i=1}^{n} v_{EO_i}$$
$$= \mu_0 \cdot \frac{1}{n} \sum_{i=1}^{n} E_i \cdot 10^{(pH_i - pK)} / [1 + 10^{(pH_i - pK)}]$$
(3)

where n is the number of segments. The electro-osmotic flow calculated according to Eq. 3 is assumed to be a plug flow and treated in the same way as the imposed flow in the previous version of the model [7]. The time dependence is given by the variability of the voltage gradient and pH. Thus, this simple approach requires μ_0 and the pK value of the wall as "specific" inputs and permits the combined simulation of the temporal behavior of electroosmosis and electrophoresis in both uniform and discontinuous buffer systems.

3. Experimental

3.1. Chemicals

The chemicals used were of analytical-reagent or research grade.

3.2. Computer simulations

The program was executed on an Excel AT 486 computer (Walz Computer, Berne, Switzerland) or a notebook 486 computer (Data 2000, Berne, Switzerland) running at 50 and 33 MHz,

Table 1
Electrochemical parameters used in simulation

Compound	pK_1	pK_2	Mobility coefficient $(10^{-8} \, m^2/V \cdot s)$
Tryptophan	2.38	9.40	2.54
Tryptamine	9.30		2.54
ACES	6.84		3.13
Na$^+$			5.19
H$^+$			36.27
OH$^-$			19.87

respectively. The component's input data for simulation are summarized in Table 1. All simulations were performed with a 5 cm separation space divided into 600 segments of equal length. For making plots, the data were imported into SigmaPlot Scientific Graphing Software version 4.01 (Jandel Scientific, Corte Madera, CA, USA) or into a software of our own design, termed 3DPLOT, which permits simple three-dimensional data presentation [7]. All plots were printed on an HP Laserprinter IIP (Hewlett-Packard, Widen, Switzerland).

3.3. Instrumentation and experimental procedure

Electrokinetic measurements were made with two instruments featuring 50 or 75 μm I.D. fused-silica capillaries which were purchased from Polymicro Technologies (Phoenix, AZ, USA) (products TSP/075/375 and TSP/050/375, respectively), a laboratory-made set-up described previously [7,9] and the Prince apparatus (Lauerlabs, Emmen, Netherlands). Prior to use, capillaries were etched with 1 M sodium hydroxide solution for about 20 min. If not stated otherwise, the capillaries were conditioned for each experiment by rinsing with running buffer for at least 10 min.

4. Results and discussion

To simulate electroosmosis in fused-silica capillaries, two specific inputs are required, a wall or absolute electroosmotic mobility (serving for the calculation of electroosmotic transport) and a wall pK describing the dissociation of silanol groups on the capillary surface (representing surface charge as a function of pH). Selection of these values is crucial and depends on the physical configuration employed. Using fused-silica capillaries and uniform buffers, the net electroosmotic mobility is known to be dependent not only on pH and wall pK according to

$$\mu_{EO} = \mu_0 \cdot 10^{(pH - pK)} / [1 + 10^{(pH - pK)}]$$
(4)

but also on capillary conditioning [10]. Thus, in order to be able to characterize the capillaries employed, a titration curve was measured. The data presented in Fig. 1A were obtained using a 50 μm I.D. capillary of 55 cm total and 45 cm effective length, 40 mM phosphate buffers in order of decreasing pH values and the Prince instrument. The temperature was kept at 35°C, a constant voltage of 20 kV was applied and the current was in the range 26–72 μA. Phosphate buffers were prepared from stock solutions of H_3PO_4, NaH_2PO_4 and Na_2HPO_4 (0.2 M each) and methanol was used as a marker substance for electroosmosis. Before each run, the capillary was flushed with running buffer for 5 min
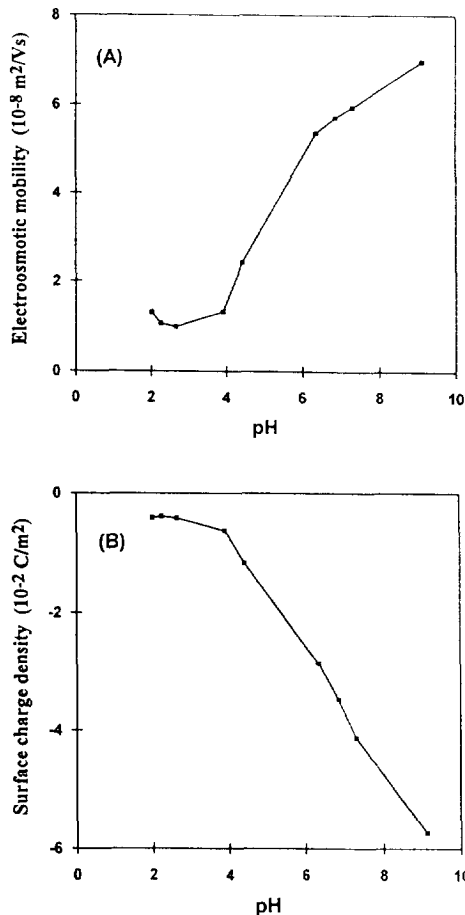

Fig. 1. Capillary titration data with (A) experimentally determined net electroosmotic mobility as a function of pH and (B) calculated surface charge density.

through application of a positive pressure of 3000 mbar. Sample application [water–methanol, (60:40)] was effected by a 20 mbar pressure for 6 s.

The pH dependence of the net electroosmotic mobility shown in Fig. 1A is comparable to that reported for a monitoring sequence in the order of decreasing buffer pH values [10]. Not surprisingly, the titration curve is characterized by a steep change in the pH 5–7 interval, this representing the dissociation of the silanol groups. Further, at low pH, the data do not reflect those expected from the vanishing dissociation of monovalent silanol [11], the residual mobility being ascribed to contributions made by anion adsorption. At high pH, a net electroosmotic mobility of larger than $6 \cdot 10^{-8}$ m^2/V·s is observed, in agreement with reported values [10].

The small mobility increase observed at pH < 3 can be ascribed to the decrease in ionic strength encountered when keeping the phosphate buffers at a constant 40 mM. Neglect of the OH$^-$ concentration and assuming electroneutrality, the ionic strength of a phosphate buffer consisting of monovalent cations (e.g. Na$^+$ and K$^+$) is given by

$$u = \frac{K_1[\mathrm{H}^+]^2 + 3K_1K_2[\mathrm{H}^+] + 6K_1K_2K_3}{[\mathrm{H}^+]^3 + K_1[\mathrm{H}^+]^2 + K_1K_2[\mathrm{H}^+] + K_1K_2K_3} \cdot C_\mathrm{P}$$

(5)

where C_P is the total phosphate concentration (M) and $K_{1,2,3}$ are the dissociation constants of phosphoric acid. The electroosmotic mobility is given by [12]

$$\mu_{\mathrm{EO}} = -\frac{\varepsilon_0 \varepsilon_\mathrm{r} \zeta}{\eta} = -\frac{\sigma}{\kappa \eta}$$

(6)

where ε_0 is the permittivity of vacuum (8.854 · 10^{-12} C^2/N·m^2), ε_r the dielectric constant of the running buffer (75 for water at 35°C), η the viscosity of the solution (0.000719 N·s/m^2 for water at 35°C), ζ the zeta potential at the capillary wall, σ the surface charge density of the capillary wall (C/m^2) and κ the Debye–Hückel parameter given by

$$\kappa^2 = \frac{2000F^2}{\varepsilon_0\varepsilon_r RT} \cdot u$$

where F is the Faraday constant (96495 C/mol) and R the universal gas constant (8.31 J/K·mol). Substitution of the ionic strength expressed by Eq. 5 in Eq. 6, rearrangement and insertion of the measured mobility values permit the calculation of the surface charge density of the capillary wall (Fig. 1B), a property which provides direct insight into the degree of ionization of the silanol groups. Again, surface charge is shown not to become zero at low pH, this being another indication of anion adsorption on the capillary wall at pH < 4. Thus, selection of a wall pK of 6, which corresponds to the pK_a value of the silanol groups [11], is unlikely to provide meaningful predictions for capillary electrophoresis in low pH buffers. For pH > 5.5, however, this could be different and was therefore investigated.

The capillary zone electrophoretic separation of tryptophan (Trp) and tryptamine (Tra) in a buffer composed of 100 mM of the weak acid N-[2-acetamido]-2-aminoethanesulfonic acid (ACES) and 90 mM NaOH was studied. Using the input parameters listed in Table 1, the pH and conductivity values of that buffer were

Fig. 2. Computer-predicted concentration profiles of Trp and Tra at 1-min intervals.

calculated to be 7.79 and 0.723 S/m, respectively. The simulation data depicted in Fig. 2 were obtained with an initial sample pulse at the anodic capillary end comprising Trp and Tra (0.5 mM each) and tenfold diluted running buffer. To simplify matters, the dynamic behavior was studied in a column of length 5 cm and with a constant applied voltage of 77.5 V (15.5 V/cm; initial current density 1000 A/m^2). For the calculation of electroosmosis, a wall pK of 6 and a mobility of $7 \cdot 10^{-8}$ m^2/V·s were employed. For that configuration, a constant electroosmotic displacement towards the cathode of 106.8 μm/s was predicted. The data presented in Fig. 2 represent the predicted dynamics of the concentration profiles of the two solutes at 1-min intervals. In this system, Tra has a positive charge with electrophoretic and electroosmotic displacements being in the same direction. Tra is predicted to reach the cathodic end of the column after about 5.2 min of power application. Trp is partially negatively charged and thus electromigrates in the opposite direction to the cathodic electroosmotic flow. The latter displacement, however, is much stronger and Trp is predicted to leave the capillary column at its cathodic end after about 7.2 min. Separation is predicted to be fairly fast with full resolution being obtained in about 1 min.

The data presented in Fig. 3 depict the detector responses predicted for UV absorbance at 220 nm. Responses for detectors placed between 20 and 80% of the column length (10% interval) are shown, the signals representing the summation of the concentrations of Trp and Tra supplemented by 0.4% of the ACES concentration, this corresponding to equal absorption of the two solutes and the much smaller absorption of ACES at a wavelength of 220 nm. The decrease in the predicted detector response originates from the buffer difference between running buffer and applied sample, a change which is monitored only at low wavelengths (Fig. 4). The three-dimensional data shown in Fig. 4 were obtained with the laboratory-made instrument equipped with a 75 μm I.D. capillary of 70 cm total and 50 cm effective length. Sampling occurred for 5 s. The applied constant voltage
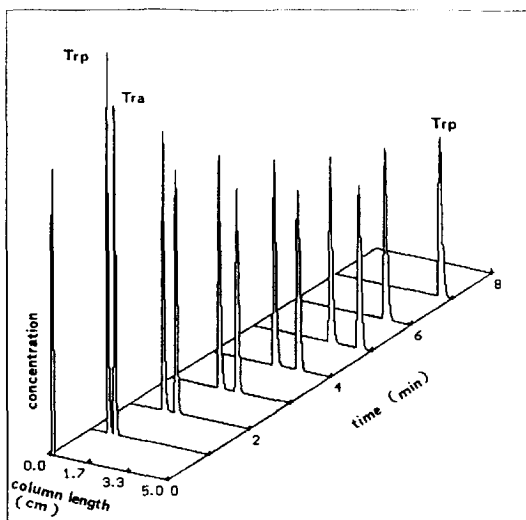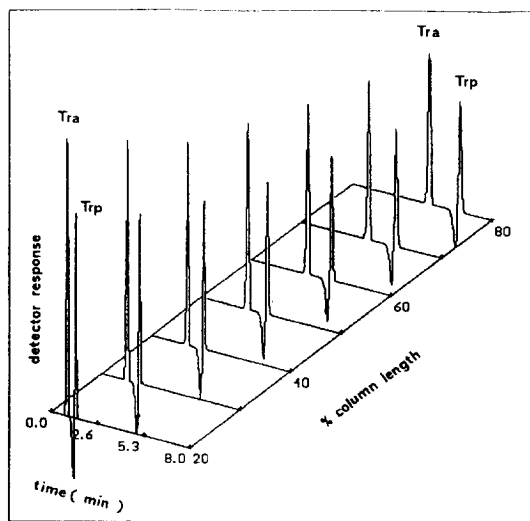
Fig. 3. Computer-predicted detector responses for detectors located between 20 and 80% of the column length (10% interval). The responses represent UV absorption at 220 nm.

was 15 kV and the sample components were dissolved in tenfold diluted running buffer. As predicted, Tra was detected first at 4.60 min after power application, whereas Trp (7.29 min) was monitored shortly after the detection of the capillary void volume at 6.93 min (marked with V). For close comparison of the simulation and experimental data, the following has to be considered. In the experiment, a voltage gradient of 214.3 V/cm was applied, this being 13.8 times larger than that employed for the simulation. On the other hand, the column length used for computer prediction was fourteen times shorter than that used experimentally. Hence the time

scales of prediction and experimental validation should be comparable. As is shown by the data presented in Fig. 5, this was essentially true. Evaluation of the experimental data revealed an electroosmotic net mobility of $5.61 \cdot 10^{-8}$ m^2/ V·s, this being about 80% compared with that employed for the simulation. Hence the experimentally determined detection time intervals are about 7.00/5.61 (the ratio of the two mobilities) longer than those predicted. For the detector profile depicted as the dashed line in Fig. 5, this difference was taken into account, and qualitative agreement between experiment and simulation was obtained. Further, the transport velocities of Tra and Trp in the simulation were significantly smaller than those in the experiment (see below). Therefore, the experimental peaks observed were sharper than those predicted (Fig. 5).

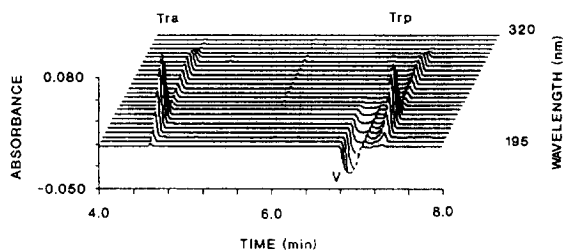The dependence of electroosmosis on ionic

Fig. 4. Three-dimensional electropherogram depicting the separation of Trp and Tra, and the travelling buffer discontinuity (V), for absorption wavelengths between 195 and 320 nm (5-nm interval).
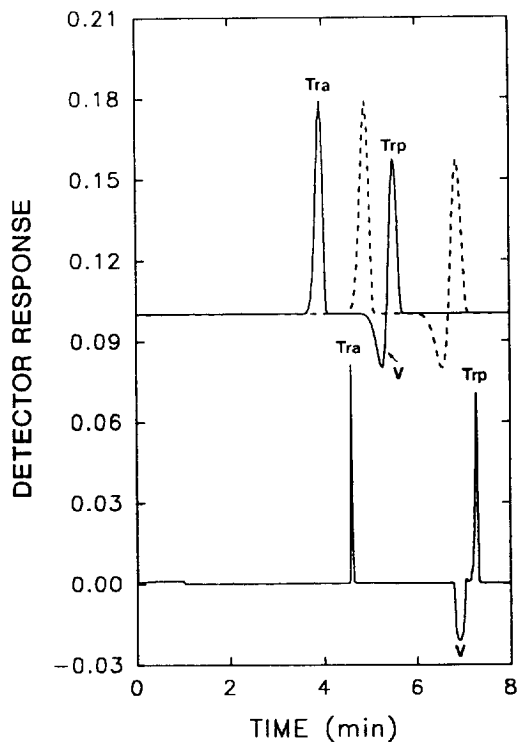

Fig. 5. Computer-predicted (top) and experimentally determined (bottom) absorption signals for a detector placed at 71.3% of the column length. For further explanation, see text.

strength is not taken into account with the present model. Electroosmosis is known to decrease as the ionic strength increases (Eq. 6 and Ref. [13]). For a buffer composed of 100 mM ACES and 90 mM NaOH (pH 7.79), the ionic strength is 89.96 mM. This is about 10% lower than the ionic strength of 103.5 mM calculated for 40 mM phosphate buffer (Fig. 1) at pH 7.79. Therefore, from this point of view, the electroosmotic mobility expected for the ACES buffer system should be higher than that with phosphate buffer. As discussed above, however, the opposite was found experimentally. Another aspect to be discussed is the impact of temperature. It is important to note that the experimental data presented in Figs. 4 and 5 were measured at ambient temperature (about 25°C), whereas the data presented in Fig. 1 were obtained at 35°C. According to Eq. 6, the surface charge is proportional to

$$\mu_{\mathrm{EO}}\eta\sqrt{\frac{u}{T}} \qquad (7)$$

where η and u are strongly and weakly, respectively, temperature dependent. Values for Eq. 7 were calculated by taking the viscosity of water at 25 and 35°C (0.8904 and 0.7194 cP, respectively), the experimentally determined mobilities for the two buffers (5.61 · 10^{-8} and 6.2 · 10^{-8} m^2/V · s (Fig. 1) for ACES and phosphate at pH 7.79, respectively), and neglecting the temperature dependence of u. The value for the ACES buffer obtained was found to be about 6% larger than that for the phosphate buffer. This similarity reveals that the surface charge mainly originates from the dissociation of the silanol groups and unlikely to be dependent on buffer composition when pH > 6. Further, temperature has a much stronger impact on electroosmosis than ionic strength. Also, the conclusion can be reached that the column conditioning for the two experimental set-ups was comparable.

For the system described, the model predicts a constant electroosmotic flow (Fig. 6). At constant voltage, the current density and column resistance, however, were determined to change as a function of time (Fig. 6). This was not only calculated by the model, but also observed
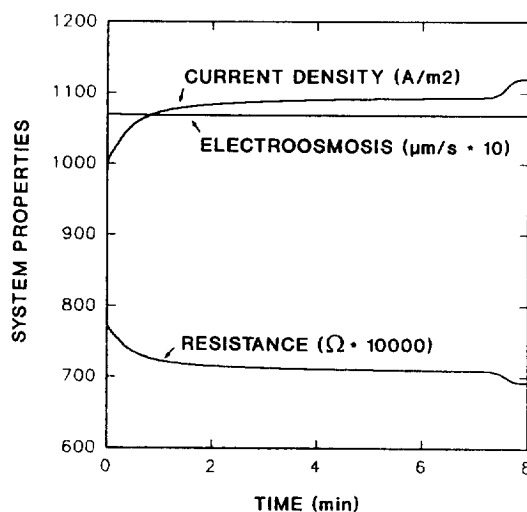

Fig. 6. Computer-predicted temporal variation of current density, resistance and electroosmosis.

experimentally, the current first increasing rapidly from 60 to 70 μA followed by a slow further increase to 75 μA. The change in these parameters is mainly attributed to the strong buffer discontinuity of the initial sampling pulse travelling through the column. Fig. 7A depicts the computer-predicted buffer change and the solute concentrations 2.5 min after power application. For the same time point, the distributions of pH, conductivity and electroosmosis are presented in Fig. 7B. The buffer discontinuity is predicted to leave the column shortly after 7 min (Fig. 3), this also being seen with the current density (resistance) increase (decrease) depicted in Fig. 6. Across the buffer change, the pH is predicted to remain almost constant, whereas the local conductivity and electroosmosis strongly change (Fig. 7B). These computer-simulated data are shown to further reveal interesting insight into the dynamics of the system's parameters which are difficult to monitor with customary absorption and fluorescence detection.

Simulation of the same zone electrophoretic separation but with the sample being applied in plain (undiluted) buffer, a configuration in which the two sample compounds are the only discontinuous elements in the column, was also investigated. With application of the same con-
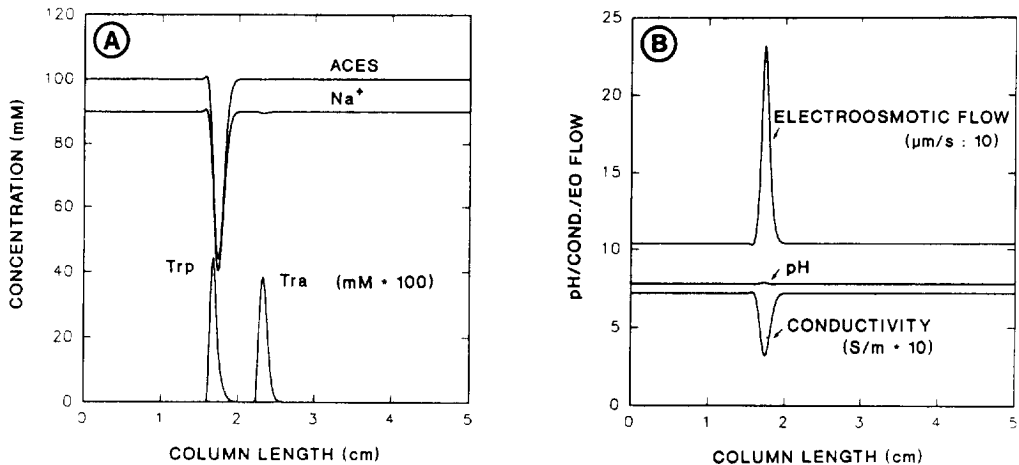
Fig. 7. Computer-predicted distributions of (A) concentrations of all components at 2.5 min of current flow and (B) pH, conductivity and electroosmosis for the same time point. For presentation, the concentrations of Trp and Tra in (A) were multiplied by 100.

stant voltage of 77.5 V, electroosmosis, current density and column resistance were calculated to be invariant, the values being 106.8 μm/s, 1120 A/m^2 and 0.0692 Ω, respectively. For the two approaches, the electroosmotic flow is predicted to be the same. This, however, does not apply to the electrical properties of the two columns. Compared with the data presented in Figs. 2–7, the configuration with plain buffer in the sample is not associated with the initial sharpening of sample components (Fig. 8) or with a buffer discontinuity travelling with the velocity of elec- troosmosis. Not surprisingly, and in agreement with prediction by the model, the absorbance decrease associated with this buffer change (marked V in Figs. 4 and 5) was not detected when Trp and Tra were sampled together with undiluted buffer (data not shown).

With the same model, emulated detector sig- nals for other detection properties, including conductivity, pH and indirect optical detection, can also be obtained. In fact, a detector response specificity to any component passing the detector can be assigned, permitting one to simulate any specific detector responses, including those ob- tained with electrochemical detection. The data presented in Fig. 9 are those for a detector placed at 71.3% of the column length, the upper
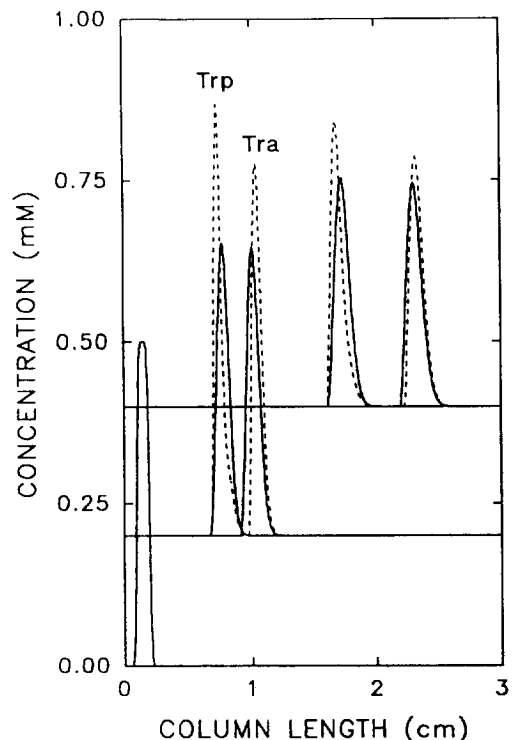

Fig. 8. Computer-simulated concentration profiles of Trp and Tra after 0, 1 and 2.5 min of current flow (from bottom to top with an offset of 0.2 mM between time points) and for the sample applied in plain buffer (solid lines) and in tenfold diluted buffer (broken lines).
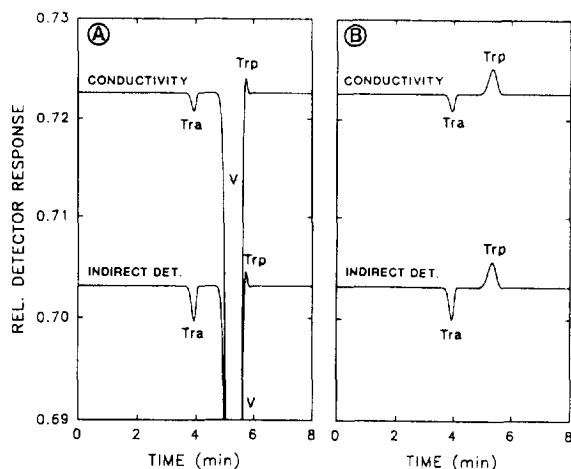
Fig. 9. Computer-predicted detector responses for conductivity (top) and indirect detection based on concentration changes of the buffer cation (Na^+, bottom) for sample applied (A) in tenfold diluted and (B) in plain buffer. The detector was placed at 71.5% of the column length. For conductivity and indirect detection, the ordinate scale represents S/m and $mM \cdot 0.00781$, respectively.

and lower graphs representing predicted responses for conductivity monitoring and indirect optical detection based on changes in the buffer cation (Na^+), respectively. Data produced by ACES changes were determined to be similar to those of Na^+ and are therefore not shown. Overall there is great similarity between the predicted responses of the two detectors. With tenfold diluted buffer in the initial sample zone (Fig. 9A), a very strong signal deviation across the travelling discontinuity (marked V) is predicted, a response which interferes considerably with the detection of Trp. Hence the use of conductivity and indirect absorbance detection cannot be recommended for compounds present within the buffer gradients originating from the initial sample buffer discontinuity. The monitoring of Tra, however, is not affected and could therefore be accessible with both detector systems. Having undiluted buffer in the sample (Fig. 9B) Tra and Trp are predicted to be detected by a signal decrease and increase, respectively.

5. Conclusions

The new model provides a realistic prediction of electroosmosis in fused-silica capillary electrophoresis. It is also capable of visualizing the whole dynamics of all components and column properties, including current density, voltage gradient and resistance. Emulated detector responses (at specified column locations) for absorbance, fluorescence, indirect optical, electrochemical, conductivity and pH detection are also obtained. It is important to realize that electroosmosis is considered to represent plug flow. Hence the predicted boundary dispersion is based solely on diffusion and electromigration. To compute electroosmosis in buffers with pH > 5.5, a wall pK of 6 and a wall mobility between $5 \cdot 10^{-8}$ and $7 \cdot 10^{-8}$ $m^2/V \cdot s$ are required to provide simulation data which are in good qualitative agreement with experimental data. This parameter selection is in agreement with titration curves, i.e., electroosmotic mobility vs. pH relationships, determined in fused-silica capillaries. For an environment with pH < 5.5, however, the same model can only be employed by specifying a wall pK lower than 6, which produces data of lower accuracy. More work is required to incorporate the impact of anions adsorbed on the capillary wall on electroosmosis. The use of the model to simulate electroosmosis in discontinuous buffers is in progress.

Acknowledgement

References

[1] M. Bier, O.A. Palusinski, R.A. Mosher and D.A. Saville, Science, 219 (1983) 1281.
[2] R.A. Mosher, D. Dewey, W. Thormann, D.A. Saville and M. Bier, Anal. Chem., 61 (1989) 362.
[3] R.A. Mosher, D.A. Saville and W. Thormann, The Dynamics of Electrophoresis, VCH, Weinheim, 1992.
[4] R.A. Mosher, P. Gebauer, J. Caslavska and W. Thormann, Anal. Chem., 64 (1992) 2991.

[5] E.V. Dose and G.A. Guiochon, Anal. Chem., 63 (1991) 1063.

[6] S.V. Ermakov and P.G. Righetti, J. Chromatogr. A, 667 (1994) 257.

[7] W. Thormann, S. Molteni, E. Stoffel, R.A. Mosher and J. Chmelík, Anal. Methods Instrum., 1 (1993) 177.

[8] R. Deshmukh and M. Bier, Electrophoresis, 14 (1993) 205.

[9] J. Caslavska, S. Lienhard and W. Thormann, J. Chromatogr., 638 (1993) 335.

[10] W.J. Lambert and D.L. Middleton, Anal. Chem., 62 (1990) 1585.

[11] J.C. Jacquier, C. Rony and P.L. Desbene, J. Chromatogr. A, 652 (1993) 337.

[12] P.D. Grossman, in P.D. Grossman and J.C. Colburn (Editors), Capillary Electrophoresis: Theory and Practice, Academic Press, San Diego, 1992, pp. 3-45.

[13] F. Foret, L. Křivánková and P. Boček, Capillary Zone Electrophoresis, VCH, Weinheim, 1993, p. 45.